# Melt State Reinforcement of Polyisoprene by Silica Nanoparticles Grafted with Polyisoprene

## Deboleena Dhara, Sanat K Kumar\*

Department of Chemical Engineering Columbia University New York, NY

## Zaid Abbas, MD Anisur Rahman, Eric Ruzicka, Brian C Benicewicz

Department of Chemistry and Biochemistry University of South Carolina Columbia, SC

### **Abstract**

We systematically vary the nanoparticle (NP) dispersion in composites formed by mixing polyisoprene homopolymers with polyisoprene grafted silica particles, and demonstrate how creep measurements allow us to overcome the limitations of small amplitude oscillatory shear (SAOS) experiments to access nearly 13 orders in time in the mechanical response of the resulting composites. We find that a specific NP morphology, a percolating particle network achieved at intermediate graft densities, significantly reinforces the system and has a lower NP percolation loading threshold relative to other morphologies. These important effects of morphology only become apparent when we combine creep measurements with SAOS reemphasizing the role of synergistically combining methods to access the mechanical properties of polymer nanocomposites.

Elastomers reinforced with nanoparticles (NPs) are important to many technologies, most prominently in improving the energy efficiency of tire technologies.<sup>1,2</sup> Typically hydrophilic NPs aggregate in a hydrophobic polymer, thus making it difficult to control their spatial dispersion in a polymer matrix.<sup>3</sup> Previously, several solutions have been proposed to address this issue in the context of elastomers, including the use of coupling agents, coating agents and functionalized polymers chains. 4-8 Such in situ approaches are strongly limited by the reaction kinetics of chains being bonded to the NP surfaces. In contrast, pregrafting polymers on the NPs helps to optimize and control dispersion by the use of parameters such as the graft density and the ratio of graft to matrix chain length. 10-13 These situations leverage the surfactancy of hydrophilic NPs being grafted with hydrophobic chains to assemble them into a variety of superstructures. In particular, Kumar et al. used a compilation of experiments and numerical simulations on conventional polymers (PS,PMMA,PEO where the graft and matrix have the same chemical composition) to delineate regions in parameter space where well dispersed, phase separated, strings, connected sheets and small clusters form. 14 Associated with these studies are experiments focused on understanding the effect of different dispersion states on mechanical properties. Nanoscale and macroscopic experiments show that a composite with percolating sheets of particles displays "gel-like" or solidlike behavior at lower particle loadings than does a composite with uniform particle dispersion. In these cases we found additional reinforcements when such particle percolated structures were accompanied by sufficient entanglement between the graft chains on adjacent NPs. 15-17

Much of the prior mechanical studies have been conducted through small amplitude oscillatory shear (SAOS), which is typically limited to a restricted frequency range and also the accompanying

range of torques necessary. Thus, while the use of the time temperature superposition (TTS) principle can expand the range of SAOS, we cannot really investigate the long time response for these composites especially in the limit of low moduli. To better understand the correlation between local structure and rheological behavior across a broad range of time scales, we need to expand the frequency range of our study – here we achieve this through the use of creep tests. 18, 19 Extending the studies to a longer time period will help us differentiate the performance of different morphologies over a wider frequency window and thereby provide additional insights to designing composites with desired properties. To better understand the reinforcement across different morphologies in filled elastomers, we ask two basic questions: (1) How are the prior findings relevant to commercially relevant elastomeric systems, where the graft and the matrix may not always have the same chemical (micro) structure? (2) Is the previous finding of improved reinforcement for percolated structures, found over limited moduli ranges, valid for more broad ranges of properties? The second question can be asked in more specific ways as (a) at a particular NP loading, do the percolated structures display improved reinforcement over the entire frequency range? and (b) Is there a threshold in the time/frequency scale beyond which the reinforcement decays and the different morphologies behave more similarly? Answering these questions will further provide insight into how these morphologies yield mechanical reinforcement, presumably through the mechanism of percolation.

In this work, we investigate the rheological response of different morphologies of polyisoprene nanocomposites using a combination of SAOS and creep measurements.<sup>18</sup> Polyisoprene grafted silica of different graft densities and chain lengths dispersed in industrial polyisoprene matrix are investigated, Table 1 [see Supporting Information].<sup>13, 20</sup>

**Table 1**: Polyisoprene Grafting Parameters

Sample	Graft chain	Grafting density	P/N	χ
	length(N)	$(\sigma)$	$1/\alpha$	
	(kDa)	(chains/nm <sup>2</sup> )		
WD	38	0.25	0.9	1.01
CN	20	0.15	1.8	0.82
S	32	0.035	1.1	0.23

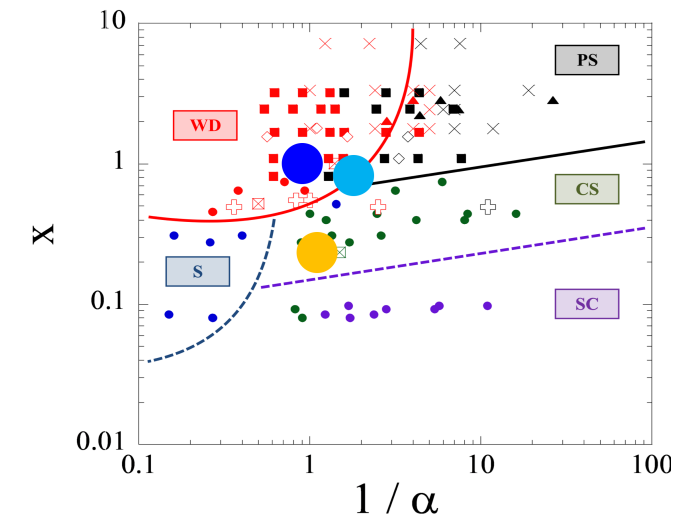


Figure 1. Morphology diagram of polymer grafted nanoparticles in a polymer matrix, borrowed from Kumar et al (WD: well dispersed, PS: phase separated, S: strings, CS: connected sheets, SC: small clusters) [R]. The y and x axis represent spherical brush overcrowding parameter (X) and the melt to brush chain length ratio ( $1/\alpha$ ). On the same plot we plot the different systems studied in this work: blue circle-well dispersed (WD), light blue-connected network (CN) and yellow-sheets (S).

Previous work has established that slight mismatches in the microstructure of the graft PI and matrix PI chains do not qualitatively affect the morphologies expected following Figure 1, which was derived for case where the graft and matrix chains of the are same microstructure.<sup>9, 10, 21</sup> To re-verify these ideas we studied the NP dispersion in three systems lying in different regions of the morphology diagram, depending on their graft density, ratio of the matrix and

graft chain length, using TEM and SAXS, Figure 1 and Figure 2. The samples lie, respectively, (i) well within the well dispersed region (dark blue, short grafted chains and moderately high grafting density), (ii) the boundary of the sheet forming region (light blue, short grafted chains and moderate grafted density), and (iii) into the sheet forming region (yellow, short grafted chains and

low grafting density). As expected, the scattering pattern for the sample in the sheet forming region (yellow; S) shows a sharp upturn at the low-q with a  $I \sim q^{-2}$  dependence. Highly agglomerated sheet-like structures can be observed in the corresponding TEM image. The dark blue sample shows uniform well dispersed (WD) particles, as expected. The sample on the boundary (light blue; CN) at intermediate graft density, although certainly containing agglomerated NPs, appears to be somewhere in between S and WD. SAXS shows scattering with a low-q scaling exponent of  $\approx 1.5$ . Visually, the NP appear to form a percolated network structure, as seen in the TEM image.

We first study the rheological behavior of these three nanocomposites in the linear regime using

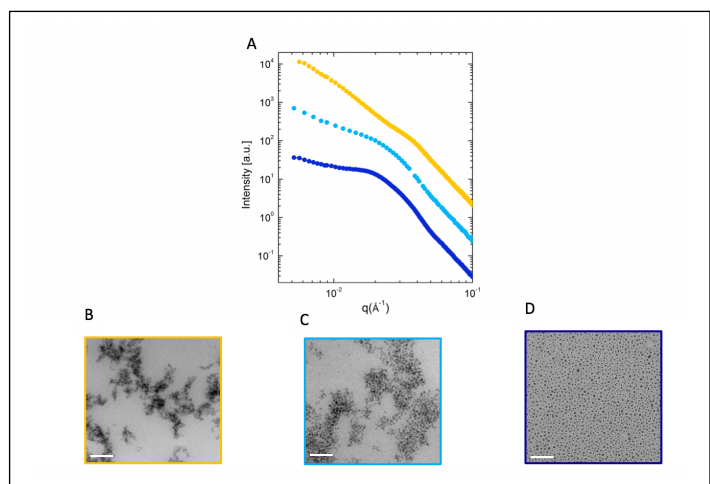


Figure 2. (A) SAXS for the three morphologies: WD (blue), CN (light blue) and S (yellow) at 5wt% NP loading. The parameters of each morphology is given in table 1, (B,C,D) Corresponding TEM images

SAOS at temperatures between -50°C and 10°C. Testing at temperatures higher than 10°C is challenging due to decreasing torque, outside the limits of the rheometer. We could of course use larger plates but we are material limited. Instead, creep experiments were performed at 0°C for different stresses.<sup>22</sup> The creep compliance data is converted

to dynamic compliance and then to dynamic moduli by a Fourier transform, thus allowing us to extend our study to lower frequencies.<sup>23, 24</sup> In the region of overlap, the converted moduli from creep and the master overlay created from oscillatory measurements superimposed perfectly, validating this method [see Supporting Information].

SAOS determined viscoelastic mastercurves in the linear regime (storage, G', and loss modulus, G'', plotted against reduced angular frequency  $a_T\omega$ ) were obtained using tTS at each NP loading and morphology (Figure 3).<sup>25-27</sup> As expected, we observe a liquid to solid transition, as evidenced by a G' plateau at low frequencies, with increased NP loading for each of the different morphologies.<sup>17</sup> This increase is typically attributed to NP-driven reinforcement due to the formation of connected NP networks beyond a percolation threshold.<sup>5, 11, 15, 28-33</sup>

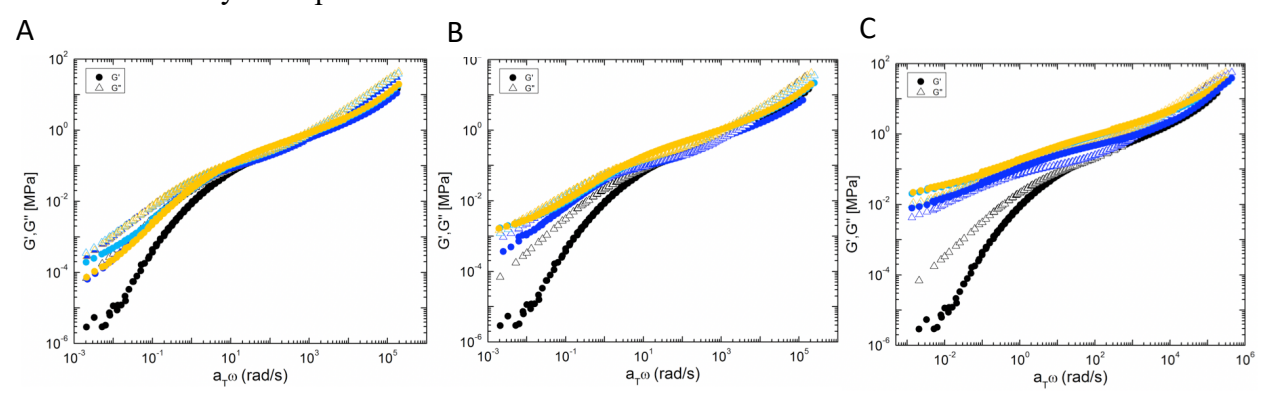


Figure 3. (A,B,C) Storage (G') and loss (G'') modulus for 5wt%, 8wt% and 15wt% NP loading in the nanocomposites, respectively. The different colors correspond to the three morphologies: WD (blue), CN (light blue) and S (yellow).

At 5wt% NP loading we observe a hint of a reinforcing plateau for CN but all the three samples clearly display liquid like behavior and appear to be below the percolation threshold. At lower loadings, the intermediate frequency entanglement plateau modulus of pure polyisoprene is unaffected, while a clear increase at 15wt% NP loading reflects the reinforcing action of NPs.<sup>28</sup> A strong entanglement plateau is not observed, presumably because the number of entanglements per chain is low.<sup>34</sup> The high frequency moduli appears unaffected with particle loading.

Comparing the reinforcement across the three morphologies, we observe that while the WD sample shows poor reinforcement there is no significant difference between CN and S. Since the SAOS measurements are not particularly illuminating, we expand the time/modulus scale of our study

through creep tests.<sup>18, 19</sup> For the neat sample a constant slope of one on a log-log plot of creep compliance as a function of time indicates that steady state is achieved, Figure 4a. With the addition of particles, we observe a decrease in slope and reduced creep compliance values at long creep times.<sup>35</sup> At 5wt% NP loading, while S and WD samples still show flow like properties, CN reaches a compliance plateau.

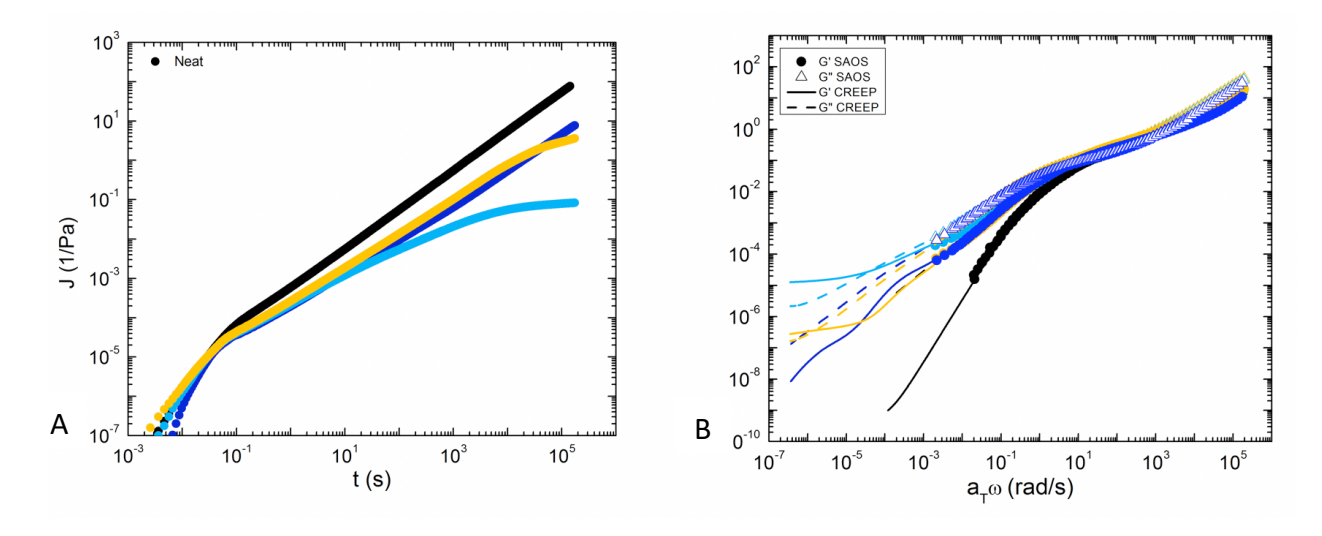


Figure 4. (A) Creep compliance for WD (blue), CN (light blue) and S (yellow) at 5% NP loading, (B) Storage (G') and loss (G'') modulus from SAOS (symbols) and creep (lines).

The linear responses derived by combining data from SAOS and creep are shown in Figure 4b. We now observe more dramatic mechanical property differences between the three morphologies. The neat polymer is a viscoelastic liquid, exhibiting a terminal flow regime scaling of  $G' \propto \omega^2$  and  $G'' \propto \omega^{.25}$  The rheological response of the WD sample from creep measurements is in line with the SAOS experiments; this material also behaves akin to a viscoelastic liquid. For the S sample, on the other hand, the storage (G') and loss (G'') modulus curves appear to be parallel to each other, implying that the sample is close to its percolation threshold at 5wt% NP loading. At low frequencies there appears to be a weak plateau with a  $G_{eq}$  value of 0.3Pa. It is difficult to measure such low modulus values from SAOS alone. The CN sample, on the other hand, shows a

reinforced equilibrium shear modulus plateau ( $G_{eq}$ ); it does not flow even after shearing the sample for 90 hours. Thus, this material behaves like a (viscoelastic) solid, i.e., it is well above it percolation threshold at 5wt% loading of the NPs, with a defined  $G_{eq}$  value of 12Pa. (For reference Moll et al estimated this value as 8Pa by extrapolating SAOS measurements with larger plates. <sup>16</sup>)

Prior work on the mechanical properties of nanocomposites shows that the appearance of a longer relaxation time at lower frequencies is more prominent for aggregated morphologies than well dispersed structures. <sup>11</sup> Moll et al. compared the reinforcement across clusters, sheets and connected network structures and noticed a non-monotonic dependence of mechanical reinforcement with changing morphologies. As mentioned above only the connected network showed a hint of a low frequency plateau. <sup>16,38</sup> In a similar study, Akcora et al showed that percolating NP sheets displayed solid-like mechanical behavior at lower particle loadings than one with uniform particle dispersion at the same NP loading. <sup>15</sup> Our results go beyond these past works by accessing lower frequencies – thus, we can clearly enunciate the relationship between NP dispersion state and mechanical reinforcement.

Our results show that maximum mechanical reinforcement occurs for the sample with intermediate grafting density, specifically the one lying at the boundary between regions with well dispersed, phase separated and sheets morphologies. This emphasizes our previous conclusion that the percolation of NPs is necessary for stress propagation and reinforcement. Mechanical reinforcement is thus driven by formation of a nanoparticle network, with the particles as the junction points and graft-graft entanglements as the elastically effective strands.<sup>16</sup>

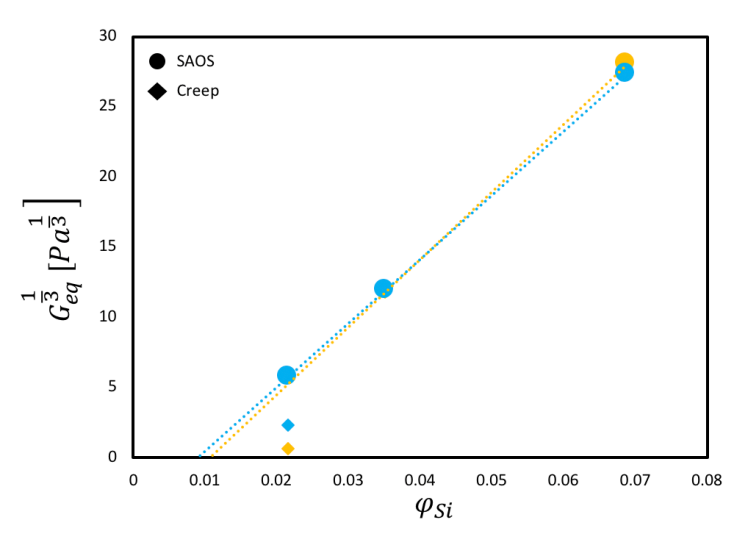


Figure 5. Cube root of  $G_{eq}$  for samples S (yellow) and CN (light blue) at different volume fractions of silica NP. The dotted lines are linear fits to the SAOS data to estimate the percolation threshold.

The onset of the percolation threshold can be quantitatively evaluated by resorting to rubber elasticity theory. Mean field rubber elasticity theory suggests that  $G_{eq} \sim (\varphi - \varphi_c)^3$ . When we plot  $G_{eq}^{\frac{1}{3}}$  versus the volume fraction of silica NPs, we can extrapolate  $G_{eq}^{\frac{1}{3}}$  down to zero to estimate the onset of gelation. If we take the  $G_{eq}$  values from SAOS alone, the onset of gelation is expected to be 2.1 wt% (1.06 vol%) and 2.5 wt% (1.1 vol%) for CN and S, respectively, and the expected value of  $G_{eq}$  for both of them is ~193Pa at 5 wt% NP loading (Figure 5). The estimation of  $G_{eq}$  and the subsequent prediction of the percolation threshold from SAOS alone disagrees with our findings from creep measurements. The extrapolated creep data at 5 wt% suggests that not only do the different morphologies percolate at different NP loadings, but that the  $G_{eq}$  values of CN and S at 5 wt% are 12Pa and 0.3Pa, respectively (Figure 5). The CN sample percolates at the lowest NP loading followed by the S and then the WD samples. The estimate of the true percolation threshold requires us to get the correct estimate of  $G_{eq}$  at all particle loadings – this can be better achieved with creep than with the use of SAOS alone. Preliminary data for S at 8 wt% loading show a  $G_{eq}$  value of 356Pa instead of the 1640Pa suggested by SAOS alone (see Supporting

Information). Longer tests are needed at higher loadings to correctly estimate the  $G_{eq}$  values. Currently, the challenges and uncertainties revolving around these long tests limit our study to lower particle loadings.

In summary, creep measurements allow us (1) access frequencies beyond the resolution of SAOS, (2) access low plateau modulus values reliably, (3) reliably measure  $G_{eq}$  values, (4) correctly predict percolation thresholds and (5) understand the difference between morphologies across a broader time scale. This is particularly useful when sample degradation or decreasing torque limits our tests to lower temperatures. Furthermore, we have shown that the formation of percolated connected networks is critical to the mechanical reinforcement of elastomeric nanocomposites. Thus, we conclude that SAOS, particularly in combination with linear creep, provides a powerful tool to study the structural impact on the rheology for filled elastomers. Understanding the melt rheology of elastomers lays the groundwork to formulating crosslinked rubber materials with desired properties, a topic of great interest to the automotive industry.

#### Materials and method:

Polymer was dissolved in THF at 5wt% and vortexed for two hours at room temperature. Polyisoprene grafted nanoparticles were added to the polymer solution at 5wt%, 8wt% and 15wt% of the nanoparticle core to the total mass. The resulting mixture was vortexed for 1 hour. Irganox was added at 0.5wt% of the polymer to prevent polymer degradation. The resulting solution was vortexed for another hour and then probe sonicated (24% of its maximum amplitude for 3 minutes, 2 seconds pulse and 1 seconds stop).

SAOS and creep measurements were carried out using DHR-3 rheometer (TA instruments). In both cases an 8mm plate-plate geometry was used. For SAOS, we performed frequency sweeps at temperatures between -50°C to 10°C. Amplitude sweep was performed at each temperature to locate the linear regime. For creep, measurements were carried out at 0°C for different stresses for over 50 hours to ensure the tests are performed in the linear regime. (see Supporting Information). Creep measurements consist of applying a constant stress, small enough to ensure linear viscoelasticity, for a given time. 40 Taking into account small uncertainties in the rheological experiments (associated with NP loading), frequency sweeps were performed before creep tests. Each test was run on a newly loaded sample. The creep compliance curves at different stresses superimpose assuring linearity and tests were performed long enough to ensure that steady state is achieved. Compliance curves were subsequently inverted to obtain G' and G'' via a multimode Maxwell fit using the software NLReg based on a generalized Tikhonov regularization.<sup>23</sup> The inverted creep was shifted to the reference temperature via time temperature superposition and combined with the mastercurves obtained from SAOS. Small angle x-ray scattering (SAXS) measurements were done using a SAXSLab Ganesha with a Cu-K  $\alpha$  source (8.04 keV photon energy, 1.5406 Å wavelength and beam size of  $200\mu m \times 200\mu m$ ).

#### **References:**

- 1. Dibbanti, M. K.; Mauri, M.; Mauri, L.; Medaglia, G.; Simonutti, R., Probing small network differences in sulfur-cured rubber compounds by combining nuclear magnetic resonance and swelling methods. *Journal of Applied Polymer Science* **2015**, *132* (43), n/a-n/a.
- 2. Mary, C.; Philippon, D.; Lafarge, L.; Laurent, D.; Rondelez, F.; Bair, S.; Vergne, P., New Insight into the Relationship Between Molecular Effects and the Rheological Behavior of Polymer-Thickened Lubricants Under High Pressure. *Tribology Letters* **2013**, *52* (3), 357-369.
- 3. Fröhlich, J.; Niedermeier, W.; Luginsland, H. D., The effect of filler–filler and filler–elastomer interaction on rubber reinforcement. *Composites Part A: Applied Science and Manufacturing* **2005**, *36* (4), 449-460.

- 4. Baeza, G. P.; Genix, A.-C.; Degrandcourt, C.; Petitjean, L.; Gummel, J.; Schweins, R.; Couty, M.; Oberdisse, J., Effect of Grafting on Rheology and Structure of a Simplified Industrial Nanocomposite Silica/SBR. *Macromolecules* **2013**, *46* (16), 6621-6633.
- 5. Baeza, G. P.; Genix, A. C.; Degrandcourt, C.; Petitjean, L.; Gummel, J.; Couty, M.; Oberdisse, J., Multiscale Filler Structure in Simplified Industrial NanocompositeSilica/SBR Systems Studied by SAXS and TEM. *Macromolecules* **2013**, *46* (1), 317-329.
- 6. Bouty, A.; Petitjean, L.; Chatard, J.; Matmour, R.; Degrandcourt, C.; Schweins, R.; Meneau, F.; Kwasniewski, P.; Boue, F.; Couty, M.; Jestin, J., Interplay between polymer chain conformation and nanoparticle assembly in model industrial silica/rubber nanocomposites. *Faraday Discuss* **2016**, *186*, 325-343.
- 7. Bouty, A.; Petitjean, L.; Degrandcourt, C.; Gummel, J.; Kwasniewski, P.; Meneau, F.; Boue, F.; Couty, M.; Jestin, J., Nanofiller Structure and Reinforcement in Model Silica/Rubber Composites: A Quantitative Correlation Driven by Interfacial Agents. *Macromolecules* **2014**, *47* (15), 5365-5378.
- 8. Stauch, C.; Ballweg, T.; Haas, K. H.; Jaeger, R.; Stiller, S.; Shmeliov, A.; Nicolosi, V.; Malebennur, S.; Wötzel, J.; Beiner, M.; Luxenhofer, R.; Mandel, K., Silanization of Silica Nanoparticles and Their Processing as Nanostructured Micro-Raspberry Powders—A Route to Control the Mechanical Properties of Isoprene Rubber Composites. *Polymer Composites* **2018**, *40* (S1).
- 9. Bonnevide, M.; Jimenez, A. M.; Dhara, D.; Phan, T. N. T.; Malicki, N.; Abbas, Z. M.; Benicewicz, B.; Kumar, S. K.; Couty, M.; Gigmes, D.; Jestin, J., Morphologies of Polyisoprene-Grafted Silica Nanoparticles in Model Elastomers. *Macromolecules* **2019**, *52* (20), 7638-7645.
- 10. Akcora, P.; Liu, H.; Kumar, S. K.; Moll, J.; Li, Y.; Benicewicz, B. C.; Schadler, L. S.; Acehan, D.; Panagiotopoulos, A. Z.; Pryamitsyn, V.; Ganesan, V.; Ilavsky, J.; Thiyagarajan, P.; Colby, R. H.; Douglas, J. F., Anisotropic self-assembly of spherical polymer-grafted nanoparticles. *Nat Mater* **2009**, *8* (4), 354-U121.
- 11. Chevigny, C.; Dalmas, F.; Di Cola, E.; Gigmes, D.; Bertin, D.; Boue, F.; Jestin, J., Polymer-Grafted-Nanoparticles Nanocomposites: Dispersion, Grafted Chain Conformation, and Rheological Behavior. *Macromolecules* **2011**, *44* (1), 122-133.
- 12. Srivastava, S.; Agarwal, P.; Archer, L. A., Tethered nanoparticle-polymer composites: phase stability and curvature. *Langmuir* **2012**, *28* (15), 6276-81.
- 13. Abbas, Z. M.; Tawfilas, M.; Khani, M. M.; Golian, K.; Marsh, Z. M.; Jhalaria, M.; Simonutti, R.; Stefik, M.; Kumar, S. K.; Benicewicz, B. C., Reinforcement of polychloroprene by grafted silica nanoparticles. *Polymer* **2019**, *171*, 96-105.
- 14. Kumar, S. K.; Jouault, N.; Benicewicz, B.; Neely, T., Nanocomposites with Polymer Grafted Nanoparticles. *Macromolecules* **2013**, *46* (9), 3199-3214.
- 15. Akcora, P.; Kumar, S. K.; Moll, J.; Lewis, S.; Schadler, L. S.; Li, Y.; Benicewicz, B. C.; Sandy, A.; Narayanan, S.; Illavsky, J.; Thiyagarajan, P.; Colby, R. H.; Douglas, J. F., "Gel-like" Mechanical Reinforcement in Polymer Nanocomposite Melts. *Macromolecules* **2010**, *43* (2), 1003-1010.
- 16. Moll, J. F.; Akcora, P.; Rungta, A.; Gong, S. S.; Colby, R. H.; Benicewicz, B. C.; Kumar, S. K., Mechanical Reinforcement in Polymer Melts Filled with Polymer Grafted Nanoparticles. *Macromolecules* **2011**, *44* (18), 7473-7477.
- 17. Zhao, D.; Ge, S. F.; Senses, E.; Akcora, P.; Jestin, J.; Kumar, S. K., Role of Filler Shape and Connectivity on the Viscoelastic Behavior in Polymer Nanocomposites. *Macromolecules* **2015**, *48* (15), 5433-5438.
- 18. Wingstrand, S. L.; Shen, B.; Kornfield, J. A.; Mortensen, K.; Parisi, D.; Vlassopoulos, D.; Hassager, O., Rheological Link Between Polymer Melts with a High Molecular Weight Tail and Enhanced Formation of Shish-Kebabs. *ACS Macro Letters* **2017**, *6* (11), 1268-1273.
- 19. Parisi, D.; Buenning, E.; Kalafatakis, N.; Gury, L.; Benicewicz, B. C.; Gauthier, M.; Cloitre, M.; Rubinstein, M.; Kumar, S. K.; Vlassopoulos, D., Universal Polymeric-to-Colloidal Transition in Melts of Hairy Nanoparticles. *ACS Nano* **2021**, *15* (10), 16697-16708.

- 20. Khani, M. M.; Abbas, Z. M.; Benicewicz, B. C., Well-defined polyisoprene-grafted silica nanoparticles via the RAFT process. *Journal of Polymer Science Part A: Polymer Chemistry* **2017**, *55* (9), 1493-1501.
- 21. Alkhodairi, H.; Russell, S. T.; Pribyl, J.; Benicewicz, B. C.; Kumar, S. K., Compatibilizing Immiscible Polymer Blends with Sparsely Grafted Nanoparticles. *Macromolecules* **2020**, *53* (23), 10330-10338.
- 22. Gabriel, C. M., H., Creep recovery behavior of metallocene linear low-density polyethylenes. *Rheologica Acta* **1999**, *38* (5), 393-403.
- 23. Weese, P., A regularization method for nonlinear ill-posed problem~. *Computer Physics Communications* **1993**, 77, 429-440.
- 24. Gabriel, C.; Kaschta, J.; Münstedt, H., Influence of molecular structure on rheological properties of polyethylenes. *Rheologica Acta* **1998**, *37* (1), 7-20.
- 25. D.Ferry, J., Viscoelastic Properties of Polymers. Third ed.; 1980.
- 26. Hiemenz, P. C.; Lodge, T. P., *Polymer Chemistry*. CRC Press: 2007.
- 27. Goad, M.; Hintzen, P.; Kahle, S.; Allgaier, J.; Richter, D.; Fetters, L., Rheological Properties of 1,4-Polyisoprene over a Large Molecular Weight Range. *Macromolecules* **2004**, *37*, 8135-8144.
- 28. Baeza, G. P.; Dessi, C.; Costanzo, S.; Zhao, D.; Gong, S.; Alegria, A.; Colby, R. H.; Rubinstein, M.; Vlassopoulos, D.; Kumar, S. K., Network dynamics in nanofilled polymers. *Nat Commun* **2016,** *7*, 11368.
- 29. Jouault, N.; Dalmas, F.; Boue, F.; Jestin, J., Multiscale characterization of filler dispersion and origins of mechanical reinforcement in model nanocomposites. *Polymer* **2012**, *53* (3), 761-775.
- 30. Jouault, N. V. P. D. F. S., S.; Jestin, J.; Boue, F., Well-Dispersed Fractal Aggregates as Filler in Polymer-Silica Nanocomposites: Long-Range Effects in Rheology. *Macromolecules* **2009**, *42*, 2031-2040.
- 31. Yang, J.; Melton, M.; Sun, R.; Yang, W.; Cheng, S., Decoupling the Polymer Dynamics and the Nanoparticle Network Dynamics of Polymer Nanocomposites through Dielectric Spectroscopy and Rheology. *Macromolecules* **2019**, *53* (1), 302-311.
- 32. Chen, Q.; Gong, S.; Moll, J.; Zhao, D.; Kumar, S. K.; Colby, R. H., Mechanical Reinforcement of Polymer Nanocomposites from Percolation of a Nanoparticle Network. *ACS Macro Letters* **2015**, *4* (4), 398-402.
- 33. Wu, S.; Qiu, M.; Tang, Z.; Guo, B., Interphase Percolation Mechanism Underlying Elastomer Reinforcement. *The Journal of Physical Chemistry C* **2017**, *121* (51), 28594-28603.
- 34. Yavitt, B. M.; Salatto, D.; Zhou, Y.; Huang, Z.; Endoh, M.; Wiegart, L.; Bocharova, V.; Ribbe, A. E.; Sokolov, A. P.; Schweizer, K. S.; Koga, T., Collective Nanoparticle Dynamics Associated with Bridging Network Formation in Model Polymer Nanocomposites. *ACS Nano* **2021**.
- 35. Muenstedt, H. K., N.; Kaschta, J., Rheological Properties of Poly(methyl methacrylate)/Nanoclay Composites As Investigated by Creep Recovery in Shear. *Macromolecules* **2008**, *41*, 9777-9783.
- 36. Winter, H. H.; Chambon, F., Analysis of Linear Viscoelasticity of a Crosslinking Polymer at the Gel Point. *Journal of Rheology* **1986**, *30* (2), 367-382.
- 37. Winter, H. H.; Chambon, F., Linear Viscoelasticity at the Gel Point of a Crosslinking PDMS with Imbalanced Stoichiometry. *Journal of Rheology* **1987**, *31*.
- 38. Moll, J.; Kumar, S. K.; Snijkers, F.; Vlassopoulos, D.; Rungta, A.; Benicewicz, B. C.; Gomez, E.; Ilavsky, J.; Colby, R. H., Dispersing Grafted Nanoparticle Assemblies into Polymer Melts through Flow Fields. *ACS Macro Letters* **2013**, *2* (12), 1051-1055.
- 39. Rubenstein, M. C., R.H., *Polymer Physics*. Oxford University Press: Oxford: UK, 2003.
- 40. <AAN009e Application of Rheology to Polymers.pdf>.